FINITE ELEMENT ANALYSIS OF A LARGE DEFORMATION ELASTO-PLASTIC CONTACT PROBLEM

by

MAKARAND S. KULKARNI

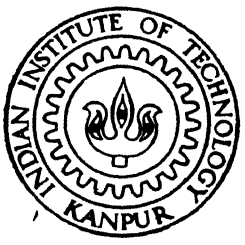

DEPARTMENT OF MECHANICAL ENGINEERING

INDIAN INSTITUTE OF TECHNOLOGY KANPUR

JULY 1997

FINITE ELEMENT ANALYSIS OF A LARGE DEFORMATION ELASTO-PLASTIC CONTACT PROBLEM

A Thesis Submitted

in Partial Fulfilment of the Requirements

for the Degree of

Master of Technology

by

MAKARAND S. KULKARNI

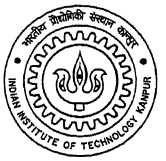

to the

DEPARTMENT OF MECHANICAL ENGINEERING

INDIAN INSTITUTE OF TECHNOLOGY KANPUR

July, 1997

CERTIFICATE

It is certified that the work contained in the thesis entitled **Finite Element Analysis of a Large Deformation Elasto-plastic Contact Problem,** by **Makarand S. Kulkarni**, has been carried out under my supervision and that this work has not been submitted elsewhere for a degree.

Dr. P. M. Dixit
Professor
Department of Mechanical Engineering
Indian Institute of Technology Kanpur

July, 1997

Acknowledgements

I, with immense pleasure express my indebtness and a deep sense of gratitude to Dr. P. M. Dixit, whose devotion and encouragement at every step with active participation enabled me to carry out this modest piece of work.

Finally, I thank my friends, in particular, Bhole, Satya, Varmaji and Atul for their cooperation and assistance throughout my stay at IIT K. I take this opportunity to thank all others who have helped me in completing this work

Makarand S. Kulkarni
IIT Kanpur
July,1997

Contents

Title ii

Certificate iii

Acknowledgements iii

Abstract iv

Contents v

List of Figures vii

Nomenclature ix

1 INTRODUCTION 1

1 1 Literature Survey 1

1.2 Objective of the Present Work 3

1.3 Structure of the thesis 4

2 Finite Element Formulation For Elasto-Plastic Deformation 5

2.1 Introduction 5

2.2 Stress and strain measures for large deformation 6

2.3 Updated Lagrangian formulation 7

2.4 Elasto-plastic model 10

2.5 Finite Element Formulation 13

2.5.1 Incremental stress-strain relationship representing material nonlinearity 13

2.5.2 Finite Element Equations 16

2.5.3 Solution Procedure 19

3 Contact Formulation **21**

3.1 Contact constraints 21

3.2 Contact Force Expressions 24

3.3 Lagrange Multiplier Method 27

3.4 Algorithm for elasto-plastic contact problem 28

4 Results and Discussion **30**

4.1 Validation of computer code 30

4.1.1 Validation for elasto-plastic part of computer code 31

4.1.2 Validation of contact part of code 33

4.2 Elasto-plastic contact problem 36

5 Conclusions and Scope for Future Work **43**

5.1 Conclusions 43

5.2 Scope for Future Work 43

Bibliography **45**

List of Figures

1.1 (a) node-to-node interface model (b) node-to-segment interface model 3

3.1 Two body contact system 22

3 2 Points in contact and associated normals 23

4.1 Simply supported beam under uniformlly distributed load . . . 31

4.2 Load ratio versus the deflection ratio 32

4.3 Load ratio versus the deflection ratio 32

4.4 A two-beam contact system (P = 80 MN) 33

4.5 A finite element mesh for the beam in contact 34

4.6 Deformed configuration of the beams in contact (Load level-15) 34

4.7 Deformed configuration of the beams in contact (Load level-30) 34

4.8 The maximum deflection of the upper beam as a function of the load level 35

4.9 The maximum deflection of the upper beam as a function of the load level 35

4.10 Contact system of a ball over a plate (R = 75.00mm, h=20.00mm) 36

4.11 Finite element mesh for the ball over plate system 37

4.12 Deformed mesh (polycarbonate-polycarbonate) 38

4.13 Maximum deflection of load point as function of load level (polycarbonates-polycarbonate) 38

4.14 Deformed mesh (acrylic-acrylic) 40

4.15 Deformed mesh (acrylic-polycarbonate) 40

4.16 Deformed mesh (polycarbonate-acrylic) 41

4.17 Maximum deflection of load point as function of load level (acrylic-acrylic) 41

4.18 Maximum deflection of load point as function of load level (acrylic-polycarbonate) 42

4.19 Maximum deflection of load point as function of load level (poylcabonate-acrylic) 42

Nomenclature

$\{a\}$	Flow vector
$[B_L]$	Matrix relating the incremental linear strain to the incremental displacement
$[B_N]$	Matrix relating the incremental non-linear strain to the incremental displacement
$[C]$	Elastic stiffness matrix
C^{EP}_{ijkl}	Elasto-plastic stiffness tensor
$[C^{EP}]$	Elasto-plastic stiffness matrix
$\mathrm{d}e_{ij}$	Green-Lagrange strain tensor
$\mathrm{d}t$	Incremental time
$\mathrm{d}u$	Incremental displacement
$\mathrm{d}\epsilon_{ij}$	Incremental natural strain tensor
$\{\mathrm{d}\epsilon\}$	Incremental natural strain vector
$\mathrm{d}\sigma_{ij}$	Incremental Cauchy stress

$\{d\sigma\}$	Incremental Cauchy stress vector
E	Young's modulus
$\{f\}$	Internal force vector
$\{F\}$	Static force vector
A	Hardening coefficient
K	hardening parameter
$[K]$	Stiffness matrix
$[K_L]$	Linear part of the stiffness matrix
$[K_{NL}]$	Non-linear part of the stiffness matrix
n	Hardening exponent
P	Penetration
ϕ_i	Shape function of the element
$[Q]$	Matrix containing the shape functions of the element
S_{ij}	Piola-Kirchoff stress tensor
S_F	Surface of the body on which the stresses are specified
S_D	Surface of the body on which the displacements are specified
t	Time
$\tilde{u}$	Displacement vector

V	Volume of the body
$\tilde{x}$	Position vector
$\Delta\eta_{ij}$	Incremental non-linear strain
ϵ^p_{eq}	Equivalent plastic starin
μ	Shear modulus
$\tilde{N}_1$	Outward normal vector
$\tilde{N}_2$, $\tilde{N}_3$	Tangential vectors
ν	Poisson's ratio
ρ	density
σ_{eq}	Equivalent stress
σ_{ij}	Cauchy stress
σ'_{ij}	Deviatoric part of σ_{ij}
$\{\sigma'\}$	Deviatoric stress vector
$\overset{\circ}{\sigma}_{ij}$	Jaumann stress rate
σ_Y	Yield stress
Ω_{ij}	Angular velocity tensor

Abstract

While solving contact problem, it is a common practice to use Hertz's expression for the contact area and a parabolic distribution of normal contact stress. However, for problem involving large deformation of elasto-plastic contact bodies, these things are not applicable. A finite element code is developed for solving 3-D large deformation elasto-plastic contact problems. Frictional effects, however, are not included. A node-to-segment interface model is used for calculating the contact stiffness matrix Contact constraints are imposed by using the Lagrange multiplier method The material and geometric nonlinearities are handled by using updated Lagrangian method with a modified Newton-Raphson scheme. The code is validated by solving some test problems. Finally a 3-D problem (of contact between a ball and plate) is solved for different combination of contacting materials to demonstrate the applicability of the method.

• • •

Chapter 1

INTRODUCTION

Any mechanical load results from an interaction between two mechanical components, when they come into contact with each other. Contact interactions, thus, exist in virtually all structural and mechanical system. Some times these interactions are intentional like in metal forming, while sometimes they are accidental like in vehicle crash.

Mechanical problems involving contacts are inherently non-linear. In large deformation problems, additional non-linearities such as geometric and material nonlinearities may creep in. By nature, contacting surfaces involve friction phenomenon. Contact is usually a dynamics phenomenon but can be analysed as a static phenomenon if inertial forces are small. The actual contacting surface, the contact forces and the displacements of the contacting surface are all unknown prior to the solution of the problem.

1.1 Literature Survey

Study of contact problems began more than hundred years ago. Newton's third law of motion and Coulomb's friction law can be considered as early milestones in contact problems. With these one could solve rigid body contact problems in global sense. With the development of science of deformable bodies, local

phenomena like stress distributions on contacting surface started receiving attention. Hertz solved static contact problem in elasticity in the 1880s (Hertz 1881,1882). He assumed contacting area to be small and contacting boundaries to be frictionless. Later on, Muskhelishvili (1975) and Gladwell (1973) solved some small deformation elastic contact problems using the analytical technique of integral equations.

With development of computers, people resorted to numerical methods. Finite element method has been the most widely used method. In earliar studies, contacting bodies were assumed to consist of linearly elastic materials and hence were assumed to undergo only small deformation. The loading was assumed to be proportional. The node-to-node contact interface model (Fig. 1 1a) was used for discretising the contact bodies and the contact conditions (or constraints) involving nodal displacements and forces were applied by modifying the combined stiffness or the flexibility matrix of the contacting bodies The investigators who used this model are Ohte (1973), Gartner (1977) (used proportional loading), Francavilla and Zienkiewicz (1979) (considered frictionless contact), Sachdeva and Ramakrishnan (1981a, 1981b) etc.

Kalkar & Randen (1979), Hung & Sauxe (1980) and Mahmound et. al. (1991) used the technique of mathematical programming for solving the frictionless small deformaton elastic contact problem. They minimised the total strain energy to find the contact area and the contact pressure distributions.

When the deformation is large, there is possibility that a pair of nodes, presently in contact, may undergo a large relative displacement. If node-to-node interface model is used, remeshing becomes necessary for carrying out the subsequent analysis. To avoid frequent remeshing, one must use the node-to-segment interface model (figure 1.1b). When a node-to-segment interface model is used, the contact conditions acquires a complex form when expressed in terms of the nodal nodal varibles To impose these conditions, an additional set of finite element equations, involving the contact stiffness matrix, needs to be developed using the principle of virtual work of the contact forces. The methods, which are used for implementing the contact constraints, are the Lagrange multi-

plier method, the penalty method and the transformation matrix. Kikuchi and Oden (1988) have provided the mathematical foundation for the Lagrange multiplier method and penalty method.

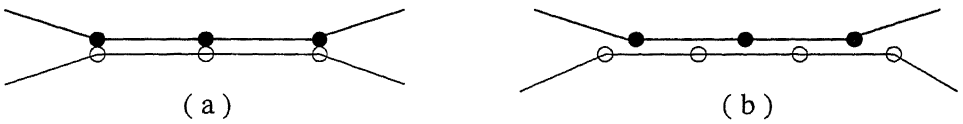

Figure 1 1: (a) node-to-node interface model (b) node-to-segment interface model

The work of Bathe & Chaudhary (1985) seems to be the first attempt to develop an expression for contact matrix using the above method. This was done for planer and axisymmetric problems assuming the contact segment to be straight. Lagrange multiplier method was used to impose the contact constraints including Coulomb's friction law. Non-linear contact kinematics was used for developing a consistent contact matrix first for 2-D problems by Wriggers & Simo (1985) and then by Parish (1989). They used both the Lagrange multiplier method and penalty method. The transformation matrix method for 2-D problems was proposed by Chen and Yeh (1988). A formulation for non-linear frictional model proposed by Gallego & Anza (1989) using perturbed Lagrangian functional. All the above formulations are for static large deformation elastic contact problem. Resently, some of these formulations have been extended to elasto-dynamic contact problem (Chaudhary and Bathe, 1990; Wriggers et al,1990) and dynamic elasto-plastic problems (Zhong, 1993)

1.2 Objective of the Present Work

The objective of the present work is to develop a simple yet reasonably accurate and efficient finite element formulation for a 3-D large-deformation elasto-plastic conatct problem without friction. Since, it is a large deformation problem, a node-to-segment interface model is used. A procedure described by Zhong(1993) is used to calculate the contact stiffness matrix because of its simplicity. Lagrange multiplier method is used to impose the contact con-

straints as penalty method is found to give reasonable solution for a limited range of penalty numbers.

Elasto-plastic behaviour is modelled by a flow rule based on von-Mises yield condition and power-law type isotropic hardening Incremental analysis is carried out using the updated Lagrangian method (Bathe, 1996). Modified Newton-Raphason method is used to solve the resulting finite element equations Contact iterations are carried out within a Newton-Raphson iteration.

A finite element code is developed which is first validated by solving some test problems Later a 3-D problem is solved to demonstrate the applicabilty of the formulation.

1.3 Structure of the thesis

The finite element formulation for Updated Lagrangian method and constitutive relationship between stress and strains for plasticity are developed in second chapter. The third chapter deals with calculation of contact forces and imposition of the contact constraints by Lagrange multiplier method. The fourth chapter deals with validation of computer code and solving ball over plate problem. The last chapter summarises the work carried out and suggests the possible further scope of the present work.

User: kms
Host: vayu
Class: vayu
Job: laser-658

Chapter 2

Finite Element Formulation For Elasto-Plastic Deformation

2.1 Introduction

When the deformation is large, displacements, strains and stresses, experienced by a body do not remain proportional to the applied load. The response of the body becomes nonlinear. The nonliearities involved in a large deformation elasto-plastic problem are of two kinds: geometric nonlinearity and material nonlinearity. For elasto-plastic materials, the Updated Lagrangian formulation is the most convenient as the stress-strain relationship for such materials is usually represented in an incremental manner.

In this chapter, first the stress and strain measures appropriate for a large deformation problem are discussed. Later incremental equations for Updated Lagrangian method are derived. To deal with the material non-linearity, elasto-plastic model based on the isotropic hardening and the von-Mises yield criteria is developed. Finally, discretised finite element equations are derived.

2.2 Stress and strain measures for large deformation

In a large deformation problem, configuration of the body changes continuously. We can't calculate Cauchy stress at time $t + \Delta t$ simply by adding the Cauchy stress at time t and the stress increment over the time Δt. Calculation of Cauchy stress at time $t + \Delta t$ must take into account the rigid body rotation of the material elements as the components of Cauchy stress change even with rigid body rotation. To deal with the above difficulty, we need to use appropriate stress and strain tensors, which do not change with rigid body rotation. Such tensors are called as objective tensors.

One of the commonly used objective stress tensors in the Updated Lagrangian formulation is the second Piola-Kirchoff stress tensor (denoted by S_{ij}). It is related to the Cauchy stres tensor (σ_{ij}) by the relation

$$ {}^{t+\Delta t}_{t}S_{ij} = \frac{{}^{t}\rho}{{}^{t+\Delta t}\rho} \left({}_{t+\Delta t}{}^{t}x_{i,m}\right) {}^{t+\Delta t}\sigma_{mn} \left({}_{t+\Delta t}{}^{t}x_{j,n}\right) \tag{2.1} $$

Here, ${}_{t+\Delta t}{}^{t}x_{i,m}$ represents the derivative of the position vector ${}^{t}\tilde{x}$ at time t with respect to the one (${}^{t+\Delta t}\tilde{x}$) at time $t + \Delta t$. Further, ${}^{t}\rho$ and ${}^{t+\Delta t}\rho$ denote densities at time t and $t + \Delta t$ respectively. The superscripts on S_{ij} and σ_{ij} represents the deformed configuration at $(t + \Delta t)$ while the subscript on S_{ij} represents reference the configuration (at t).

The corresponding work conjugate strain tensor is the Green-Lagrange strain tensor defined by

$$ {}^{t+\Delta t}_{t}e_{ij} = \frac{1}{2}\left({}^{t+\Delta t}_{t}u_{i,j} + {}^{t+\Delta t}_{t}u_{j,i} + {}^{t+\Delta t}_{t}u_{k,i}\,{}^{t+\Delta t}_{t}u_{k,j}\right) \tag{2.2} $$

where ${}^{t+\Delta t}_{t}u_{i,j}$ is the derivative of the displacement vector at time $t + \Delta t$ with respect to the position vector at time t.

In Eulerian formulation, where the rate of deformation tensor (symmetric part of the velocity gradient tensor) is used as the deformation measure, Jaumann

stress rate tensor ($\overset{\circ}{\sigma}_{ij}$) is used as the objective tensor. However, even in the Updated Lagrangian formulation, one can use $\overset{\circ}{\sigma}_{ij}\ \Delta t$ as the incremental objective tensor. This tensor is related to Cauchy stress $\dot{\sigma}_{ij}$ by the following relation.

$$\overset{\circ}{\sigma}_{ij}\ \Delta t = \dot{\sigma_{ij}}\Delta t - \sigma_{ik}(\Omega_{jk}\Delta t) - \sigma_{jk}(\Omega_{ik}\Delta t) \tag{2.3}$$

where the incremental rotation tensor ($\Omega_{ij}\Delta t$) is given by

$$\Omega_{ij}\Delta t = \frac{1}{2}(\Delta u_{i,j} - \Delta u_{j,i}). \tag{2.4}$$

and $\Delta_t u$ represents the incremental displacement at time t

2.3 Updated Lagrangian formulation

In Lagrangian formulation, we follow the particles of the body in their motion, from the original to the final configuration of the body. One can find stresses and strains, either with reference to the original configuration, called the total Lagrangian formulation or with reference to the current configuration, called the Updated Lagrangian formulation. For an elasto-plastic problem, the Updated Lagrangian formulation is more convenient to use. This formulation [Bathe 1996], used in the present work is described in this section.

Vitual work expression at time $t+\Delta t$ for N bodies in contact can be expressed as follows

$$\sum_{n=1}^{N} \int_{t+\Delta t V} {}^{t+\Delta t}\sigma_{ij}\ \delta({}^{t+\Delta t}\epsilon_{ij})\ d^{t+\Delta t}V = {}^{t+\Delta t}\overline{\mathcal{R}} \tag{2.5}$$

where,

$$\begin{aligned} {}^{t+\Delta t}\overline{\mathcal{R}} \ = \ & \sum_{n=1}^{N} \int_{t+\Delta t S_f} \delta\left({}^{t+\Delta t}u_i^s\right)\ {}^{t+\Delta t}f_i^s\ d^{t+\Delta t}S + \\ & \sum_{n=1}^{N} \int_{t+\Delta t S_c} \delta\left({}^{t+\Delta t}u_i^c\right)\ {}^{t+\Delta t}f_i^c\ d^{t+\Delta t}S \end{aligned} \tag{2.6}$$

Here, ${}^{t+\Delta t}\sigma_{ij}$ is the Cauchy stress tensor at time $t+\Delta t$, $\delta\left({}^{t+\Delta t}\epsilon_{ij}\right)$ is the virtual infinitesimal strain tensor at time $t+\Delta t$. $\delta^{t+\Delta t}u$ is the virtual displacement at time $t+\Delta t$ and ${}^{t+\Delta t}V$ is the domain at time $t+\Delta t$. ${}^{t+\Delta t}S_f$ is the part of the boundary on which the external forces act while ${}^{t+\Delta t}S_c$ is the contact boundary. The first term of ${}^{t+\Delta t}\overline{\mathcal{R}}$ denotes the virtual work done by the applied forces while the second term is the virtual work done by the contact forces.

For further derivations, the summation sign is omitted. The major difficulty in solving the above equation is that the configuration at time $t+\Delta t$ is unknown. In the Updated Lagrangian formulation, the virtual work expression is transformed to an integral over the known domain at time t, using the second Piola-Kirchoff stress tensor and the Green-Lagrange strain tensor.

Thus, the virtual work expresion becomes

$$\int_{{}^tV} {}^{t+\Delta t}_{t}S_{ij}\,\delta({}^{t+\Delta t}_{t}e_{ij})\,d^tV = {}^{t+\Delta t}\overline{\mathcal{R}}. \tag{2.7}$$

The second Piola-Kirchoff stress tensor can be decomposed as

$${}^{t+\Delta t}_{t}S_{ij} = {}^{t}_{t}S_{ij} + \Delta_t S_{ij} \tag{2.8}$$

where, using equation 2.1, we can write

$${}^{t}_{t}S_{ij} = {}^{t}\sigma_{ij} \tag{2.9}$$

Thus,

$${}^{t+\Delta t}_{t}S_{ij} = {}^{t}\sigma_{ij} + \Delta_t S_{ij} \tag{2.10}$$

Further, the Green-Lagrange strain tensor can be decomposed into linear and nonlinear increments as follows.

$$\delta\,{}^{t+\Delta t}_{t}e_{ij} = \delta\Delta_t\epsilon_{ij} + \delta\Delta_t\eta_{ij} \tag{2.11}$$

where (from equation 2.2),

$$\Delta_t\epsilon_{ij} = \frac{1}{2}\left(\Delta_t u_{i,j} + \Delta_t u_{j,i}\right) \tag{2.12}$$

$$\Delta_t\eta_{ij} = \frac{1}{2}\left(\Delta_t u_{k,i}\right)\left(\Delta_t u_{k,j}\right). \tag{2.13}$$

Here, $\Delta_t u_{i,j}$ stands for the derivative of $\Delta_t \tilde{u}$ (incremental displacement vector at time t) with respect to ${}_t\tilde{x}$ (positon vector at time t). Thus, equation (2.7) can be written with incremental decomposition as

$$\int_{tV} \Delta_t S_{ij}\delta(\Delta_t\epsilon_{ij})\, d^tV + \int_{tV} \Delta_t S_{ij}\delta(\Delta_t\eta_{ij})\, d^tV + \int_{tV} {}^t\sigma_{ij}\delta(\Delta_t\eta_{ij})\, d^tV + \int_{tV} {}^t\sigma_{ij}\delta(\Delta_t\epsilon_{ij})\, d^tV = {}^{t+\Delta t}\overline{\mathcal{R}}. \quad (2.14)$$

The 2nd integral on the left hand side is a higher order term compared to other terms and hence can be neglected. Using appropriate constitutive relation $\Delta_t S_{ij}$ can be approximated as

$$\Delta_t S_{ij} = {}_tC_{ijkl}\ \Delta_t\epsilon_{kl} \quad (2.15)$$

Thus, equation 2.14 can be written as

$$\int_{tV} {}_tC_{ijkl}\ \Delta_t\epsilon_{kl}\delta(\Delta_t\epsilon_{ij})\, d^tV + \int_{tV} {}^t\sigma_{ij}\delta(\Delta_t\eta_{ij})\, d^tV + \int_{tV} {}^t\sigma_{ij}\delta(\Delta_t\epsilon_{ij})\, d^tV = {}^{t+\Delta t}\overline{\mathcal{R}} \quad (2.16)$$

Above equation can be employed to calculate the incremental displacement at time $t + \Delta t$, which then can be used to evaluate the incremental strain and stress. However, when these incremental displacement and stress are added to the their corresponding values at time t, it is observed that the total displacement and stress at time $t + \Delta t$ do not satisfy the virtual work equation (equation 2 5). That is, the internal virtual work (left hand side) dosen't match with the external virtual work(right hand side). This out of balance virtual work occures as a result of linearisation performed. In order to reduce this out of balance virtual work, we need to perform an iteration in which the above solution steps are repeated until we reach a convergence. The equation 2.16 then can be put in the iterative form as follows. In the k-th iteration, the equation becomes

$$\int_{t+\Delta t V^{k-1}} {}^{t+\Delta t}C^{k-1}_{ijkl}(\Delta_{t+\Delta t}\epsilon^k_{kl})\,\delta(\Delta_{t+\Delta t}\epsilon^k_{ij})\, d^{t+\Delta t}V + \int_{t+\Delta t V^{k-1}} {}^{t+\Delta t}\sigma^{k-1}_{ij}\,\delta(\Delta_{t+\Delta t}\eta^k_{ij})\, d^{t+\Delta t}V + \int_{t+\Delta t V^{k-1}} {}^{t+\Delta t}\sigma^{k-1}_{ij}\delta(\Delta_{t+\Delta t}\epsilon^{k-1}_{ij})\, d^{t+\Delta t}V = {}^{t+\Delta t}\overline{\mathcal{R}} \quad (2.17)$$

The displacements in an iteration are updated as follows

$$^{t+\Delta t}u_i^k = {}^{t+\Delta t}u_i^{k-1} + \Delta u_i^k \quad , \quad {}^{t+\Delta t}u^0 = {}^t u \tag{2.18}$$

For the first iteration, the stresses, the strains and the constitutive tensors of the previous increment are used. thus

$$^{t+\Delta t}\sigma_{ij}^0 = {}^t\sigma_{ij}^0, \quad \Delta_{t+\Delta t}\epsilon_{ij}^0 = \Delta_t\epsilon_{ij}, \quad {}_{t+\Delta t}C_{ijkl}^0 = {}_tC_{ijkl} \tag{2.19}$$

Equation 2.17 corresponds to Newton-Raphson iterations. In present analyses, the stiffness matrix (i.e. the first two terms on the left side) is not updated during the iterations, which helps in reducing the computational time. Such iterations are called modified Newton-Raphson iterations.

2.4 Elasto-plastic model

As stresses developed in a material exceed the yield stress, the linear relationship between stress and strain no longer remains valid. We now develop relationship between stress and strain based on the von-Mises yield criteria and isotropic hardening.

For an isotropic hardening material, plastic potential is given by, (Owen and Hinton, 1980)

$$F(\sigma_{ij}, p) = \sigma_{eq}(\sigma_{ij}) - \sigma_y(p) \tag{2.20}$$

Note that

$$F = 0 \tag{2.21}$$

represents the yield criterion. The plastic potential F depends on the Cauchy stress tensor σ_{ij} through it's second invariant σ_{eq} called as equivalent stress and defined by

$$\sigma_{eq} = (\frac{3}{2}\sigma_{ij}^{'}\sigma_{ij}^{'})^{\frac{1}{2}} \tag{2.22}$$

where $\sigma_{ij}^{'}$ is the deviatoric part of σ_{ij}. Further, F depends on the variable yield stress of the material, σ_y , through a hardening varible p. For the case of

strain hardening, p is identified as the equivalent plastic strain ϵ^p_{eq}, and hence defined as :

$$p = \epsilon^p_{eq} = \int \mathrm{d}\epsilon^p_{eq} \tag{2.23}$$

and

$$\mathrm{d}\epsilon^p_{eq} = (\frac{2}{3}\mathrm{d}\epsilon^p_{ij}\mathrm{d}\epsilon^p_{ij})^{\frac{1}{2}} \tag{2.24}$$

Here, $\mathrm{d}\epsilon^p_{ij}$ is the plastic part of the incremental strain tensor $\mathrm{d}\epsilon_{ij}$ and the integration in equation 2.23 is to be carried along the particle path. The dependence of σ_y on p (or ϵ^p_{eq})is normally approximated by a power-law type of relationship

$$\sigma_y = K(\epsilon^p_{eq})^n \tag{2.25}$$

Here, K is called the hardening coefficient and n is called as the hardening exponent.

The incremental plastic strain $(\mathrm{d}\epsilon^p_{ij})$ is obtained from the plastic potential using the following relation :

$$\mathrm{d}\epsilon^p_{ij} = \mathrm{d}\lambda\frac{\partial F}{\partial \sigma_{ij}} \tag{2.26}$$

where $\mathrm{d}\lambda$ is a scalar. This equation is called as the flow rule. Differentiation of equation 2.20 with respect to σ_{ij} gives

$$\frac{\partial F}{\partial \sigma_{ij}} = \frac{3}{2\sigma_{eq}}\sigma'_{ij} \tag{2.27}$$

Using this one can determine $\mathrm{d}\lambda$ as.

$$\mathrm{d}\lambda = \mathrm{d}\epsilon^p_{eq} \tag{2.28}$$

Further, the hardening relationship and the yield condition (eq. 2.25) can be used to express $\mathrm{d}\lambda$ as :

$$\mathrm{d}\lambda = \frac{\mathrm{d}\sigma_y}{H} = \frac{\mathrm{d}\sigma_{eq}}{H} \tag{2.29}$$

where

$$H = \frac{\mathrm{d}\sigma_y}{\mathrm{d}\epsilon^p_{eq}}, \tag{2.30}$$

the slope of the hardening curve, can be obtained from equation 2.25. Substitution of equations 2.27 and 2.30 in equation 2.26 leads to the following constitutive equation

$$d\epsilon_{ij}^{p} = \frac{3}{2}\frac{d\sigma_{eq}}{H\sigma_{eq}}\sigma_{ij}^{'} \tag{2.31}$$

This constitutive relationship between the deviatoric stress tensor and the incremental plastic strain tensor is not really convenient for the Updated Lagrangian formulation for which the incremental stress-strain relationship is needed. This can be obtained from equation 2.31 as follows:

$$d\epsilon_{ij}^{p} = \frac{3}{2}\frac{\sigma_{ij}^{'}}{H\sigma_{eq}}\frac{\partial\sigma_{eq}}{\partial\sigma_{kl}}d\sigma_{kl} \tag{2.32}$$

Note that, from equations 2.20 and 2.26, we get

$$\frac{\partial\sigma_{eq}}{\partial\sigma_{kl}} = \frac{\partial F}{\partial\sigma_{kl}} = \frac{3}{2\sigma_{eq}}\sigma_{kl}^{'}. \tag{2.33}$$

Substitution of equation 2.32 in equation 2.33 leads to the following incremental plastic stress-strain relationship :

$$d\epsilon_{ij}^{p} = \frac{9\sigma_{ij}^{'}\sigma_{kl}^{'}}{4H\sigma_{eq}^{2}}d\sigma_{kl}. \tag{2.34}$$

The incremental elastic stress strain relationship is given by

$$d\epsilon_{ij}^{e} = \frac{1}{E}[-\nu d\sigma_{kk}\delta ij + (1+\nu)d\sigma_{ij}] \tag{2.35}$$

where $d\epsilon_{ij}^{e}$ is the elastic part of $d\epsilon_{ij}$, E is the Young's modulus and ν is the Poisson's ratio. Adding the two relationships, we get

$$\begin{aligned} d\epsilon_{ij} &= d\epsilon_{ij}^{e} + d\epsilon_{ij}^{p} \\ &= \left[-\frac{\nu}{E}\delta_{ij}\delta_{kl} + \frac{(1+\nu)}{E}\delta_{ik}\delta_{jl} + \frac{9\sigma_{ij}^{'}\sigma_{kl}^{'}}{4H\sigma_{eq}^{2}}\right] d\sigma_{kl} \end{aligned} \tag{2.36}$$

This is the incremental elasto-plastic stress-strain relationship needed in the Updated Lagrangian formulation. However, it is the following inverse relationship which is more useful :

$$d\sigma_{ij} = C_{ijkl}^{EP}d\epsilon_{kl} \tag{2.37}$$

where

$$C^{EP}_{ijkl} = 2\mu \left[\delta_{ik}\delta_{jl} + \frac{\nu}{1-2\nu}\delta_{ij}\delta_{kl} - \frac{9\mu\sigma'_{ij}\sigma'_{kl}}{2(3\mu+H)\sigma^2_{eq}} \right] \tag{2.38}$$

and μ is the shear modulus related to E and ν by the relation:

$$\mu = \frac{E}{2(1+\nu)} \tag{2.39}$$

Note that, in equation 2.37, $d\sigma_{ij}$ cannot be interpreted as the incremental Cauchy stress tensor. Instead, it has to be identified as an increment of one of the objective stress tensors defined in section 2.2.

2.5 Finite Element Formulation

In this section, first the incremental elasto-plastic stress-strain relationship is put in a vector form Then, the incremental equation for the Updated Lagrangian formulation is put in matrix a form. Finally, these equations are expressed in terms of nodal unknowns using suitable approximation for incremental displacement field.

2.5.1 Incremental stress-strain relationship representing material nonlinearity

Since the stress-strain realtionship is path dependent for an elastic-plastic material, it is convenient to represnt it in incremental form. The incremental stress-strain relation is expressed in vector form as

$$\{d\sigma\} = [C^{EP}]\{d\epsilon\} \tag{2.40}$$

where

$$\{d\sigma\}^T = \{d\sigma_{xx}, d\sigma_{yy}, d\sigma_{zz}, d\sigma_{xy}, d\sigma_{yz}, d\sigma_{zx}\} \tag{2.41}$$

and

$$\{d\epsilon\}^T = \{d\epsilon_{xx}, d\epsilon_{yy}, d\epsilon_{zz}, 2d\epsilon_{xy}, 2d\epsilon_{yz}, 2d\epsilon_{zx}\} \tag{2.42}$$

are respectively the vector forms of the incremental (objective) stress and strain tensors The expression for the elastic-plastic matrix $[C^{EP}]$ is derived from the plastic potential F. For its derivation, it is convenient to express the yield condition (eqs. 2.20 and 2.21) as

$$F(\{\sigma\},p) \equiv \sigma_{eq}(\{\sigma\}) - \sigma_y(p) = 0 \tag{2.43}$$

where

$$\{\sigma\}^T = \{\sigma_{xx}, \sigma_{yy}, \sigma_{zz}, \sigma_{xy}, \sigma_{yz}\sigma_{zx}, \} \tag{2.44}$$

On the yield surface, $dF = 0$ and hence

$$(\frac{\partial F}{\partial\{\sigma\}})^T\{d\sigma\} + \frac{\partial F}{\partial p}dp = 0 \tag{2.45}$$

or

$$\{a\}^T\{d\sigma\} - Ad\lambda = 0 \tag{2.46}$$

where, the flow vector $\{a\}$ is defined by

$$\{a\} = \frac{\partial F}{\partial\{\sigma\}}, \tag{2.47}$$

the parameter A is given by

$$A = -\frac{1}{d\lambda}\frac{\partial F}{\partial p}dp, \tag{2.48}$$

and $d\lambda$ is the same scalar which appears in equation 2.26. Equation 2.27 gives the following expression for the flow vector:

$$\{a\} = \frac{3}{2\sigma_{eq}}\{\sigma\}'. \tag{2.49}$$

where $\{\sigma\}'$ is the vector form of the deviatoric part of σ_{ij}.
Equations 2.23 and 2.28 give

$$dp = d\lambda = d\epsilon^p_{eq}. \tag{2.50}$$

Substitution of equations 2.43 and 2.50 in equation 2.48 leads to the following expression for A:

$$A = \frac{d\sigma_y}{dp} = \frac{d\sigma_y}{d\epsilon^p_{eq}} \tag{2.51}$$

The total strain increment, after splitting into elastic and plastic parts, can be written in terms of the incremental stress vector by using the vector forms of the elastic stress-strain relationship (2.35) and flow rule(2.26) . Thus,

$$\begin{aligned}\{d\epsilon\} = \{d\epsilon^e\} + \{d\epsilon^p\} &= [C]^{-1}\{d\sigma\} + d\lambda\frac{\partial F}{\partial\{\sigma\}} \\ &= [C]^{-1}\{d\sigma\} + d\lambda\{a\} \end{aligned} \tag{2.52}$$

Here, $[C]$ is the matrix form of the elasticity tensor C_{ijkl} . Premultiplying both sides of equation 2.52 by $\{a\}^T[C]$ and using equation 2.46 , we get

$$d\lambda = \frac{\{a\}^T[C]\{d\epsilon\}}{A + \{a\}^T[C]\{a\}} \tag{2.53}$$

Substituting the above expression for $d\lambda$ in equation 2.52 we get

$$\{d\epsilon\} = [C]^{-1}\{d\sigma\} + \frac{\{a\}^T[C]\{d\epsilon\}}{A + \{a\}^T[C]\{a\}}\{a\} \tag{2.54}$$

which leads to

$$\{d\sigma\} = \left([C] - \frac{[C]\{a\}\{a\}^T[C]}{A + \{a\}^T[C]\{a\}}\right)\{d\epsilon\} \tag{2.55}$$

Therefore,

$$[C]^{EP} = \left([C] - \frac{[C]\{a\}\{a\}^T[C]}{A + \{a\}^T[C]\{a\}}\right) \tag{2.56}$$

where the definitions of a and A are given by 2.49 and 2.51. For a material with power strain hardening law (equation 2.25), the expression (2.51) for A reduces to

$$A = K\,n(\epsilon^p_{eq})^{n-1} \tag{2.57}$$

For an isotropic material, the expression for $[C]$ for the 3-dimensional case is given by

$$[C] = \frac{E}{(1+\nu)(1-2\nu)}\begin{bmatrix} 1-\nu & \nu & \nu & 0 & 0 & 0 \\ \nu & 1-\nu & \nu & 0 & 0 & 0 \\ \nu & \nu & 1-\nu & 0 & 0 & 0 \\ 0 & 0 & 0 & \frac{1-2\nu}{2} & 0 & 0 \\ 0 & 0 & 0 & 0 & \frac{1-2\nu}{2} & 0 \\ 0 & 0 & 0 & 0 & 0 & \frac{1-2\nu}{2} \end{bmatrix} \tag{2.58}$$

As stated before, $\{d\sigma\}$ has to be interpreted as an increment of one of the objective stress tensors defined in section 2.2.

2.5.2 Finite Element Equations

For developing the finite element equations, equation 2.17 need to be put in a matrix form. For notational convenience, equation 2.16 is used instead of 2.17 for this purpose. Once finite element equations corresponding to equation 2.16 are derived , the equation corrsponding to 2.17 can be obtained by carrying out the appropriate notational change. Owing to the symmetries in ${}_tC^{EP}_{ijkl}$, $\Delta_t\epsilon_{ij}$, $\Delta_t\eta_{ij}$ and σ^t_{ij}, equation 2.16 can be rewritten in the following matrix form:

$$\int_{{}_tV}\left(\delta\{\Delta_t\epsilon\}^T\right){}_t[C^{EP}]\{\Delta_t\epsilon\}d^tV + \int_{{}_tV}\left(\delta\{\Delta_t\eta\}^T\right){}^t[T]\{\Delta_t\eta\}\ \mathrm{d}^tV + \int_{{}_tV}\left(\delta\{\Delta_t\epsilon\}^T\right){}^t\{\sigma\}\ \mathrm{d}^tV = {}^{t+\Delta t}\overline{\mathcal{R}}. \quad (2.59)$$

where,

$${}_t\{\Delta\epsilon\} = \{\Delta_t\epsilon_{xx}, \Delta_t\epsilon_{yy}, \Delta_t\epsilon_{zz}, 2\Delta_t\epsilon_{xy}, 2\Delta_t\epsilon_{yz}, 2\Delta_t\epsilon_{zx}\}^T \quad (2.60)$$

$${}^t\{\sigma\} = \{{}^t\sigma_{xx}, {}^t\sigma_{yy}, {}^t\sigma_{zz}, {}^t\sigma_{xy}, {}^t\sigma_{yz}, {}^t\sigma_{zx}\}^T \quad (2.61)$$

$${}_t\{\Delta\eta\} = \{\Delta_t u_{,x}, \Delta_t u_{,y}, \Delta_t u_{,z}, \Delta_t v_{,x}, \Delta_t v_{,y}, \Delta_t v_{,z}, \cdots\}^T \quad (2.62)$$

$${}^t[T] = \begin{bmatrix} {}^t[\Sigma] & 0 & 0 \\ 0 & {}^t[\Sigma] & 0 \\ 0 & 0 & {}^t[\Sigma] \end{bmatrix} \quad (2.63)$$

and

$${}^t\left[\Sigma\right] = \begin{bmatrix} {}^t\sigma_{xx} & {}^t\sigma_{xy} & {}^t\sigma_{xz} \\ {}^t\sigma_{yx} & {}^t\sigma_{yy} & {}^t\sigma_{yz} \\ {}^t\sigma_{zx} & {}^t\sigma_{zy} & {}^t\sigma_{zz} \end{bmatrix} \quad (2.64)$$

The ${}_t[C]^{EP}$ matrix is the elastic-plastic matrix evaluated at time t which is given by equation 2.56.

The domain is discretised into a number of elements and the incremental displacement field over a typical element e is approximated as

$${}_t\{\Delta u\} = [Q]\ {}_t\{\Delta u\}^e \quad (2.65)$$

where,

$${}_t\{\Delta u\}^e = \{\Delta_t u^1, \Delta_t v^1, \Delta_t w^1, \Delta_t u^2, \Delta_t v^2, \cdots\cdots\}.$$

Here, $\Delta_t u^i$, $\Delta_t v^i$,$\Delta_t w^i$ stand for the (unknown) incremental displacements of node 'i' in x , y and z directions respectively and

$$[Q] = \begin{bmatrix} \{Q_1\}^T \\ \{Q_2\}^T \\ \{Q_3\}^T \end{bmatrix} \tag{2.66}$$

where

$$\begin{aligned} \{Q_1\}^T &= \begin{bmatrix} \Phi_1 & 0 & 0 & \Phi_2 & 0 & 0 & \Phi_3 & \dots \end{bmatrix}, \\ \{Q_2\}^T &= \begin{bmatrix} 0 & \Phi_1 & 0 & 0 & \Phi_2 & 0 & 0 & \dots \end{bmatrix}, \\ \{Q_3\}^T &= \begin{bmatrix} 0 & 0 & \Phi_1 & 0 & 0 & \Phi_2 & 0 & \dots \end{bmatrix} \end{aligned} \tag{2.67}$$

and Φ_i, the functions of (x,y,z), are called the *shape functions.*

With displacement field defined by equation 2.65, the strain field within the element can be calculated in terms of nodal displacements.

$$\Delta_t u_{i,j} = \frac{\partial \Delta_t u_i}{\partial_t x_j} = {}_t\{Q_i\}^T_{,j} \, {}_t\{\Delta u\}^e \tag{2.68}$$

where

$${}_t\{Q_i\}^T_{,j} = \frac{\partial \{Q_i\}^T}{\partial_t x_j}. \tag{2.69}$$

Substituting equation 2.68 in equations 2.12 and 2.13 and arranging them in vector form, we get the strain displacement relations:

$${}_t\{\Delta\epsilon\} = {}_t[B_L] \, {}_t\{\Delta u\}^e, \tag{2.70}$$

$${}_t\{\Delta\eta\} = {}_t[B_N] \, {}_t\{\Delta u\}^e \tag{2.71}$$

where,

$${}_t[B_L] = \begin{bmatrix} {}_t\{Q_1\}^T_{,x} \\ {}_t\{Q_2\}^T_{,y} \\ {}_t\{Q_3\}^T_{,z} \\ {}_t\{Q_2\}^T_{,x} + {}_t\{Q_1\}^T_{,y} \\ {}_t\{Q_3\}^T_{,y} + {}_t\{Q_2\}^T_{,z} \\ {}_t\{Q_1\}^T_{,z} + {}_t\{Q_3\}^T_{,x} \end{bmatrix} \tag{2.72}$$

and

$$ {}_t[B_N]^T = \{\ {}_t\{Q_1\}^T_{,x}\ \ {}_t\{Q_1\}^T_{,y}\ \ {}_t\{Q_1\}^T_{,z}\ \ {}_t\{Q_2\}^T_{,x}\ \ {}_t\{Q_2\}^T_{,y}\ \cdots\ \} \tag{2.73} $$

Using the strain displacement relations derived above, the contribution to the integral (eq. 2.59) from a typical element e (with volume ${}^tV_e$) can be written as

$$ \begin{aligned} \delta_t\{\Delta u\}^{eT} \left(\int_{{}^tV_e} {}_t[B_L]^T\ {}_t[C^{EP}]\ {}_t[B_L]\ \mathrm{d}^tV \right)\ {}_t\{\Delta u\}^e + \\ \delta_t\{\Delta u\}^{eT} \left(\int_{{}^tV_e} {}_t[B_N]^T\ [T]^t\ {}_t[B_N]\ \mathrm{d}^tV \right)\ {}_t\{\Delta u\}^e + \\ \delta_t\{\Delta u\}^{eT} \left(\int_{{}^tV_e} {}_t[B_L]^T\ \{\sigma\}^t\ \mathrm{d}^tV \right) = \delta_t\{\Delta u\}^{eT}\ ({}_{t+\Delta t}\{F\}^e) \end{aligned} \tag{2.74} $$

Here, the contribution to the term ${}^{t+\Delta t}\overline{\mathcal{R}}$ from the element e has been expressed in terms of the elemental external force vectors ${}_{t+\Delta t}\{F\}^e$ using a standard procedure (Note that ${}_{t+\Delta t}F^e$ includes both the applied as well as contact force). Since the variation in the incremental displacement vector $\delta_t\{\delta u\}^e$ is arbitrary and expressing the term within Ist parenthesis as linear elemental stiffness $[\,K_L\,]^e$ and that of 2nd one as nonlinear elemental stiffness $[\,K_{NL}\,]^e$ the above equation can be written as

$$ ({}_t[K_L]^e + {}_t[K_{NL}]^e)\ {}_t\{\Delta u\}^e + {}_t\{f\}^e = {}_{t+\Delta t}\{F\}^e \tag{2.75} $$

or

$$ {}_t[K]^e\ {}_t\{\Delta u\}^e + {}_t\{f\}^e = {}_{t+\Delta t}\{F\}^e. \tag{2.76} $$

where

$$ {}_t\{f\}^e = \int_{{}^tV_e} {}_t[B_L]^T\ {}^t\{\sigma\}\ \mathrm{d}^tV. \tag{2.77} $$

is the internal force vector at time t.

Assembling the elemental matrices $[K]^e$ and the elemental vectors ${}_t\{f\}^e$ and ${}_{t+\Delta t}\{F\}^e$ over all the elements, we get the following global equation :

$$ {}_t[K]\ {}_t\{\Delta u\}\ +\ {}_t\{f\}\ =\ {}_{t+\Delta t}\{F\}. \tag{2.78} $$

Here ${}_t[K]$ is the global stiffness matrix, ${}_t\{\Delta u\}$ is the global incremental displacement vector (at time t) and ${}_t\{f\}$ and ${}_{t+\Delta t}\{F\}$ are the global internal and

external force vectors respectively. Here, contribution to ${}^{t+\Delta t}F$ comes from both the applied forces as well as contact forces. Calculation of contact forces is discussed in next chapter.

Equation 2.76 is the finite element version of equation 2.16. If, instead of equation 2.16 , equation 2.17 is used, the corresponding finite element equation, for k-th iteration, becomes

$$ {}_{t+\Delta t}[K]^{k-1}{}_{t}\{\Delta u\}^{k} = {}_{t+\Delta t}\{F\} - {}_{t+\Delta t}\{f\}^{k-1} \tag{2.79} $$

In k-th iteration, the stiffness matrix ${}_{t+\Delta t}[K]^{k-1}$ and the internal force vector ${}_{t+\Delta t}\{f\}^{k-1}$ are calcualted using the stresses of $(k-1)$-th iteration and carrying out the integration over the updated volume of $(k-1)$-th iteration . Strictly speaking ${}_{t+\Delta t}\{F\}$ is also needs to be updated as the surfaces over which the applied and contact forces act also change.

2.5.3 Solution Procedure

As stated before, modified version of the Newton-Raphason method is used in this work. In this version, the stiffness matrix is not updated during the iterations. Thus, the solution procedure can be discussed as follows.

In the current increment, first the stiffness matix is calculated based on the stress tensor obtained at the end of the the previous increment i.e. ${}^{t}\sigma_{ij}$. This stiffness matrix is not changed till all the iterations of the current increment are over. For the first iteration of the current increment, ${}_{t+\Delta t}\{f\}^{0}$ is calculated using ${}^{t+\Delta t}\sigma^{0}_{ij} = {}^{t}\sigma_{ij}$. Then equation 2.79 is solved, using the values of external and contact forces at time $t+\Delta t$ to find $\{\Delta u\}^{1}$. Then, incremental strain is calculated from equation 2.70 and incremental stress is determined using the relation

$$ {}_{t+\Delta t}\{\Delta\sigma\}^{1} = \int_{\Delta t}[C]^{EP}\{\mathrm{d}\epsilon\}^{1} \tag{2.80} $$

Where the integration is carried out using Euler Forward integration[Bathe,1990].

This is considered as the incremental Jaumann stress, $\overset{\circ}{\sigma}{}^{1}_{ij}\ \Delta t$. From this incremental Cauchy stress $\dot{\sigma}^{1}_{ij}\ \Delta t$ is calculated using equation 2.3 and 2.4. This increment is added to ${}^{t}\sigma_{ij}$ to get ${}^{t+\Delta t}\sigma^{1}_{ij}$. Next, the geometry and ${}_{t+\Delta t}\{F\}$ are updated using incremental displcement. Using the updated geometry and ${}^{t+\Delta t}\sigma^{1}_{ij}$, the internal force vector ${}_{t+\Delta t}\{f\}^{1}$ is calculated. Using ${}_{t+\Delta t}\{F\} - {}_{t+\Delta t}\{f\}^{1}$ as the new right hand side, ${}_{t}\{\Delta u\}^{2}$ is obtained as the solution of equation 2.79. Now the incremental displacement becomes

$$ {}_{t}\{\Delta u\} = {}_{t}\{\Delta u\}^{1} + {}_{t}\{\Delta u\}^{2} \tag{2.81} $$

In the second iteration, internal force vector ${}_{t+\Delta t}\{f\}^{2}$ is calculated from ${}_{t+\Delta t}\{\Delta u\}^{2}$ using the procedure of previous paragraph . Further, ${}_{t+\Delta t}\{F\}$ is updated based on the geometric changes corresponding to ${}_{t}\{\Delta u\}^{2}$. Using ${}_{t+\Delta t}\{F\} - \{f\}^{2}$ as the right hand side, now ${}_{t}\{\Delta u\}^{3}$ is determined by solving equation 2.79. The procedure is continued till the internal and external force vectors match within a tolerance, at which point iterations are stopped. This indicates that equilibrium has been achieved in the current increment. Then the calculation for next increment begins.

Chapter 3

Contact Formulation

The quintessential part of a contact problem is to find the contact forces. The difficulty is, along the contact boundary, neither displacement nor force boundary conditions are specified. To find the contact forces, we have to impose certain contact constraints.

In this chapter, first the contact constraints are discussed. Then, the expressions for contact forces are derived using appropriate discretization of the contact boundary. Later, Lagrange multiplier method is discussed for imposing the contact constraints. Finally, the algorithm for large deformation elasto-plastic contact problem is described.

3.1 Contact constraints

A typical two body contact system is shown in Fig 3.1. The bodies occupy the domains ${}^{t+\Delta t}\bar{V}^1$ and ${}^{t+\Delta t}\bar{V}^2$ at time $t+\Delta t$. The boundaries of ${}^{t+\Delta t}\bar{V}^1$ and ${}^{t+\Delta t}\bar{V}^2$ are denoted by ${}^{t+\Delta t}S^1$ and ${}^{t+\Delta t}S^2$ and their interior volumes by by ${}^{t+\Delta t}V^1$ and ${}^{t+\Delta t}V^2$ respectively.

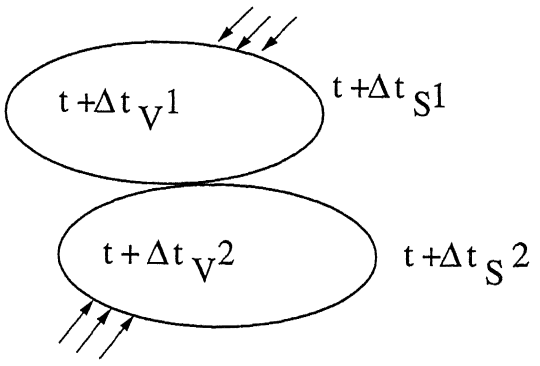

Figure 3.1: Two body contact system

At any time $t+\Delta t$, the boundary of contact body n (n =1,2) can be partitioned as

$$^{t+\Delta t}S^n = {}^{t+\Delta t}S^n_D \cup {}^{t+\Delta t}S^n_F \cup {}^{t+\Delta t}S^n_C \tag{3.1}$$

where,

$^{t+\Delta t}S_D$ = boundary where displacements are specified
$^{t+\Delta t}S_F$ = boundary where forces are specified
$^{t+\Delta t}S_C$ = boundary where contact occurs

Assuming the boundary $^{t+\Delta t}S^n$ to be smooth, outward unit normal vector at point $^{t+\Delta t}\tilde{x}^n$ on the boundary $^{t+\Delta t}S^n$ is denoted by $^{t+\Delta t}\tilde{N}^n_1$. Other two orthonormal boundary vectors are $^{t+\Delta t}\tilde{N}^n_2$ and $^{t+\Delta t}\tilde{N}^n_3$. (See Fig. 3.2)

Suppose that two boundary points $^{t+\Delta t}\tilde{x}^1$ and $^{t+\Delta t}\tilde{x}^2$ are in contact with each other at time $t+\Delta t$ and the contact traction at $^{t+\Delta t}\tilde{x}^n$ is denoted as $^{t+\Delta t}\tilde{T}^n_c$. Then by Newton's third law of motion, we have

$$^{t+\Delta t}\tilde{T}^1_c = -^{t+\Delta t}\tilde{T}^2_c \tag{3.2}$$

where $^{t+\Delta t}\tilde{T}^n_c$ can be expressed as

$$^{t+\Delta t}\tilde{T}^n_c = \sum_{i=1}^{3} {}^{t+\Delta t}t^n_i \; {}^{t+\Delta t}\tilde{N}^n_i \tag{3.3}$$

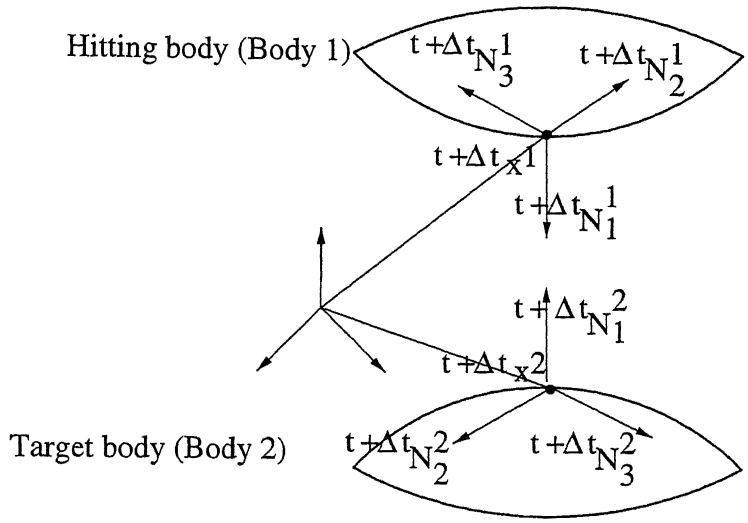

Figure 3.2: Points in contact and associated normals

Here, ${}^{t+\Delta t}t_i^n$ denote the components of ${}^{t+\Delta t}\tilde{T}_c^n$ in the direction of ${}^{t+\Delta t}\tilde{N}_i^n$.

If the two contact boundaries are not to be welded together, then the normal component of the contact traction cannot be tensile. Thus, we have

$$ {}^{t+\Delta t}t_1^n \leq 0 \tag{3.4} $$

This represents the traction constraint on the contact boundary. Besides the above condition, there are other types of constraints. Physical cosiderations require that particles of one body can't penetrate the other body. Thus, for points in contact, penetration must be zero. This condition can be mathematically stated as

$$ {}^{t+\Delta t}p = ({}^{t+\Delta t}\tilde{x}^2 - {}^{t+\Delta t}\tilde{x}^1) \cdot {}^{t+\Delta t}\tilde{N}_1^2 = 0 \tag{3.5} $$

where ${}^{t+\Delta t}p$ is the penetration or gap between the points in contact. This condition is called as the kinematic constraint.

3.2 Contact Force Expressions

As the contacting bodies are discretised for the purpose of developing finite element equations, the contact boundary gets automatically divided into surface elements, called as contact segments. While discretising the bodies, a node-to-segment interface model is used as the present work deals with a large deformation contact problem. Normally in a contact formulation, contact is considered only at discrete nodes. Here, it is assumed that a node of the hitting body (body 1) comes into contact with a segment of the target body (body 2). The first step in the development of the contact force expression is the determination of the unit normal and tangent vectors at a point on the target segment. This is described in the next paragraph.

Geometry of a target segment can be described using 2-D shape functions. Thus,

$$^{t+\Delta t}\tilde{x}^2(\xi,\eta) = \sum_{j=1}^{j=N} \Phi_j(\xi,\eta)\,^{t+\Delta t}\tilde{x}_j^2 \tag{3.6}$$

where $\Phi_j(\xi,\eta)$ are the shape functions and $^{t+\Delta t}\tilde{x}_j^2$ denote the nodal position vectors.

The side of the segment on which contact can occur is refered to as positive side of the segment and the other side as negative side of the segment. The local numbering of nodes on a contact segment should always be counter clockwise when we face the positive side of the segment. This is to get the correct sense for the outward normal vector at a given point. A normal vector at a point $^{t+\Delta t}\tilde{x}(\xi,\eta)$ on the positive side of segment is defined as

$$^{t+\Delta t}\tilde{\tilde{N}}_1 = {}^{t+\Delta t}\tilde{N}_\xi^2 \times {}^{t+\Delta t}\tilde{N}_\eta^2 \tag{3.7}$$

where, $^{t+\Delta t}\tilde{N}_\xi^2$ and $^{t+\Delta t}\tilde{N}_\eta^2$ are two tangent vectors at $^{t+\Delta t}\tilde{x}^2(\xi,\eta)$ given by,

$$^{t+\Delta t}\tilde{N}_\xi^2 = {}^{t+\Delta t}\tilde{x}^2(\xi,\eta)_{,\xi} \tag{3.8}$$

$$^{t+\Delta t}\tilde{N}_\eta^2 = {}^{t+\Delta t}\tilde{x}^2(\xi,\eta)_{,\eta} \tag{3.9}$$

The unit normal and tangent vectors are defined as

$$^{t+\Delta t}\tilde{N}_1^2 = {}^{t+\Delta t}\tilde{N}_1^2 / |^{t+\Delta t}\tilde{\tilde{N}}_1^2| \tag{3.10}$$

$$^{t+\Delta t}\tilde{N}_2^2 = {}^{t+\Delta t}\tilde{N}_\xi^2 / |^{t+\Delta t}\tilde{N}_\xi^2| \tag{3.11}$$

$$^{t+\Delta t}\tilde{N}_3^2 = {}^{t+\Delta t}\tilde{N}_\eta^2 / |^{t+\Delta t}\tilde{N}_\eta^2| \tag{3.12}$$

Since contact is considered only at discrete hitting nodes, we deal only with point forces at discrete hitting nodes rather than with distributed contact tractions. At time $t+\Delta t$, the $\{^{t+\Delta}F^2\}$ be an array of the cartisian components of the point force vector $^{t+\Delta t}\tilde{F}^2$ at a point of the target segment at which the hitting node makes the contact. By Newton's third law, the force vector on the hitting node body will be $-\{^{t+\Delta t}F^2\}$. Let $\{\delta^{t+\Delta t}u^2\}$ and $\{\delta^{t+\Delta t}u^1\}$ be the virtual displacement vectors (at time $t+\Delta t$) at these points (on the target and hitting bodies respectively) when they come in contact. Then the virtual work at hitting node can be expressed as

$$\delta w_c = \{\delta^{t+\Delta t}u^2 - \delta^{t+\Delta t}u^1\}^T \{^{t+\Delta t}F^2\} \tag{3.13}$$

Note that the elements of $\{\delta^{t+\Delta t}u^1\}$, namely $\delta^{t+\Delta t}u^1$, $\delta^{t+\Delta t}v^1$, $\delta^{t+\Delta t}w^1$ are the (virtual) nodal displacements of the hitting node. The elements of $\{\delta^{t+\Delta t}u^2\}$ can be expressed in terms of the (virtual) nodal displacements of the target segment ($\delta^{t+\Delta t}u_i^2$, $\delta^{t+\Delta t}v_i^2$, $\delta^{t+\Delta t}w_i^2$, $i = 1, \cdots N$) using 2-D shape functions (ϕ_i $i = 1, N$). Thus

$$\{\delta^{t+\Delta t}u^2 - \delta^{t+\Delta t}u^1\} = [Q_c]\{\delta^{t+\Delta t}u_c\} \tag{3.14}$$

where

$$Q_c = \begin{bmatrix} -1 & 0 & 0 & \Phi_1 & 0 & 0 & \Phi_2 & 0 & 0 & \cdots & \Phi_N & 0 & 0 \\ 0 & -1 & 0 & 0 & \Phi_1 & 0 & 0 & \Phi_2 & 0 & \cdots & 0 & \Phi_N & 0 \\ 0 & 0 & -1 & 0 & 0 & \Phi_1 & 0 & 0 & \Phi_2 & & 0 & 0 & \Phi_N \end{bmatrix} \tag{3.15}$$

and

$$\{\delta^{t+\Delta t}u_c\}^T = \{\delta^{t+\Delta t}u^1, \delta^{t+\Delta t}v^1, \delta^{t+\Delta t}w^1, \delta^{t+\Delta t}u_1^2, \delta^{t+\Delta t}v_1^2, \delta^{t+\Delta t}w_1^2, \cdots\cdots, \delta^{t+\Delta t}w_N^2\} \tag{3.16}$$

The vector $\{^{t+\Delta t}F^2\}$ can be expressed as

$$\{^{t+\Delta t}F^2\} = \begin{bmatrix} ^{t+\Delta t}N^2_{11} & ^{t+\Delta t}N^2_{21} & ^{t+\Delta t}N^2_{31} \\ ^{t+\Delta t}N^2_{12} & ^{t+\Delta t}N^2_{22} & ^{t+\Delta t}N^2_{32} \\ ^{t+\Delta t}N^2_{13} & ^{t+\Delta t}N^2_{23} & ^{t+\Delta t}N^2_{33} \end{bmatrix} \begin{Bmatrix} ^{t+\Delta t}f^2_1 \\ ^{t+\Delta t}f^2_2 \\ ^{t+\Delta t}f^2_3 \end{Bmatrix} \tag{3.17}$$

or

$$\{^{t+\Delta t}F^2\} = [^{t+\Delta t}N^2]\{^{t+\Delta t}f^2\} \tag{3.18}$$

Where $^{t+\Delta t}N^2_{ij}$ represents the j-th cartesian component of the unit vector $^{t+\Delta t}\tilde{N}^2_i$ and $^{t+\Delta t}f^2_i$ are the components, with respect to $^{t+\Delta t}\tilde{N}^2_i$, of the contact force vector $^{t+\Delta t}\tilde{F}^2$. Combining equations 3.13, 3.14 and 3.18 we get the following expressions for the virtual work at the hitting node:

$$\delta w_c = \{\delta^{t+\Delta t}u_c\}^T \{^{t+\Delta t}r_c\} \tag{3.19}$$

The vector $\{^{t+\Delta t}r_c\}$ at the hitting node is given by

$$\{^{t+\Delta t}r_c\} = [Q_c]^T [^{t+\Delta t}N^2]\{^{t+\Delta t}f^2\} \tag{3.20}$$

The vector $\{^{t+\Delta t}r_c\}$ can be split as a contribution from normal contact forces and tangential contact forces. Thus

$$\{^{t+\Delta t}r_c\} = \{^{t+\Delta t}r_n\} + \{^{t+\Delta t}r_f\} \tag{3.21}$$

Where

$$\{^{t+\Delta t}r_n\} = [Q_c]^T \{^{t+\Delta t}N^2_1\}^{t+\Delta t}f^2_1 \tag{3.22}$$

and

$$\{^{t+\Delta t}r_f\} = [Q_c]^T (\{^{t+\Delta t}N^2_2\}^{t+\Delta t}f^2_2 + \{^{t+\Delta t}N^2_3\}^{t+\Delta t}f^2_3) \tag{3.23}$$

Here the arrrays $\{^{t+\Delta t}N^2_i\}$, $i = 2,3$ contains the cartesian components of the vector $^{t+\Delta t}\tilde{N}^2_i$.

Before discussing the method of determining the contact forces, it is necessary to express the kinematic constraint in terms of the nodal displacements. The matrix form of equation 3.5 is

$$^{t+\Delta t}p = \{^{t+\Delta t}N^2_1\}^T \{^{t+\Delta t}x^2 - ^{t+\Delta t}x^1\} \tag{3.24}$$

Note that

$$\{^{t+\Delta t}x^2 - {}^{t+\Delta t}x^1\} = \{^t x^2 - {}^t x^1\} + \{\Delta_t u^2 - \Delta_t u^1\} \tag{3.25}$$

where the second term on the right hand side is an array of the Cartesian componenets of the difference of the incremental displacement vectors of the target and hitting bodies at the contact node. Analogous to equation 3.14 this can be written as

$$\{\Delta_t u^2 - \Delta_t u^1\} = [Q_c]\{\Delta_t u_c\} \tag{3.26}$$

where the vector

$$\{\Delta_t u_c\}^T = \{\Delta_t u^1,\ \Delta_t v^1,\ \Delta_t w^1,\ \Delta_t u_1^2,\ \Delta_t v_1^1,\ \Delta_t w_1^2,\ \cdots,\ {}_t w_N^2\} \tag{3.27}$$

contains the nodal values of the incremental displacement of the hitting node and the nodes of the target segment. Recognizing the first term of the right hand side of equation 3.25 as ${}^t p$ (penetration at time t), equation 3.25 now can be written as

$${}^{t+\Delta t}p = {}^t p + \{^{t+\Delta t}N_1^2\}^T\ [Q_c]\{{}_t\Delta u_c\} \tag{3.28}$$

3.3 Lagrange Multiplier Method

In Lagrange's method, the contact forces are considered as primary unknowns and the kinematic contact constraint is enforced exactly. In the present work, the contact problem is considered as frictionless. Thus contact force has only one component, namely, normal force component. Now equation 3.20 becomes

$$\{^{t+\Delta t}r_c\} = [Q_c]^T\ \{^{t+\Delta t}N_1^2\}\ {}^{t+\Delta t}f_1^2 \tag{3.29}$$

The kinematic constraint corresponding to the normal contact force is that the penetration should be zero. Thus, from equation 3.28, we have

$$\{^{t+\Delta t}N_1^2\}^T\ [Q_c]\{\Delta_t u_c\} + {}^t p = 0 \tag{3.30}$$

Combining equations 3.29 and 3 30, we obtain

$$\begin{bmatrix} 0 & \{^{t+\Delta t}q\} \\ \{^{t+\Delta t}q\}^T & 0 \end{bmatrix} \begin{Bmatrix} \{\Delta_t u_c\} \\ {}^{t+\Delta t}f_1^2 \end{Bmatrix} = \begin{Bmatrix} \{^{t+\Delta t}r_c\} \\ -{}^{t}p \end{Bmatrix} \tag{3.31}$$

where

$$^{t+\Delta t}\{q\}^T = [Q_c]^T \{^{t+\Delta t}N_1^2\} \tag{3.32}$$

For L contacting nodes, there will be L such equations. Assembling these equations, we get the following global equation.

$$\begin{bmatrix} 0 & [^{t+\Delta t}Q] \\ [^{t+\Delta t}Q]^T & 0 \end{bmatrix} \begin{Bmatrix} \{\Delta_t U_c\} \\ \{^{t+\Delta t}F_1^2\} \end{Bmatrix} = \begin{Bmatrix} \{^{t+\Delta t}R_c\} \\ -\{^{t}P\} \end{Bmatrix} \tag{3.33}$$

This equation is combined with equation 3.79 of chapter 2 to find the nodal displacement vector (which contains the vector $\{\Delta_t U_c\}$ of the contact displacements) and the contact force vector $\{^{t+\Delta t}F_1^2\}$. Note that the vector $\{^{t+\Delta t}R_c\}$ is a part of the vector $_{t+\Delta t}\{F\}$ on the right hand side of equation.

3.4 Algorithm for elasto-plastic contact problem

For solving a typical elasto-plastic contact problem, the following steps are used.

1. Contact searching: Contact node searching is carried out to find the potential nodes that (for both hitting and target bodies) may come in contact with the application of incremental load. The contact searching is carried out using a master and slave algorithm (Zhong 1993).

2. Renumbering of nodes: Nodes for the hitting and the target bodies are renumbered such that contact nodes are numbered first. This is carried

out to facilitate static condensation of stiffness matrix which helps in reducing computational time.

3. Stiffness matrix: Based on the current geomentry and state of stress stiffness matrix is calculated.

4. Newton Raphason iteration: Newton-Raphason iteration counter is initialised as $i = 1$.

5 Initial penetration: Initial penetration ${}^{t+\Delta t}p^i$ (${}^{t+\Delta t}p^0 = {}^tp$) is found using current geometry.

6. Contact iterations: Within Newton-Raphason iteration contact iterations are carried out to find the actual nodes in contact. The constrant ${}^{t+\Delta t}f_1^2 < 0$ (which is similar to equation 3.4) is used to determine whether the assumed node is in contact or not. The, displacements and contact forces are calculated after the convergence of contact iterations.

7. Updating: Displacements, stresses and the contact forces are updated.

8. Convergence: Newton-Raphason iterations are checked for convergence as described in chapter-2. If convergence is achieved then equilibrium state is reached else we have to go to step 5 and iterate till we get convergence.

Chapter 4

Results and Discussion

A 3-D finite element code is developed for a large deformation elasto-plastic frictionless contact problem based on the formulation given in chapter-2 and chapter-3. 8-noded brick elements are used for discribing the contacting bodies. 8-point Gauss Legendre numerical scheme is used for evaluating the stiffness matrix. Convergence tolerance used is 1% on the global force vector. First some test problems are solved for validating the code. Later a problem of ball over a plate is solved, to demonstrate the applicabilty of the methos.

4.1 Validation of computer code:

Validation of code is carried out in two steps

1. Validation for a large deformation elasto-plastic single body problem.
2. Validation for a large deformation elastic frictionless contact problem.

4.1.1 Validation for elasto-plastic part of computer code

The elasto-plastic part of the computer code has been validated with a theoritical example given in Chakrabarty (1987). The problem consist of a simply supported beam with uniformaly distributed load(figure 4.1).

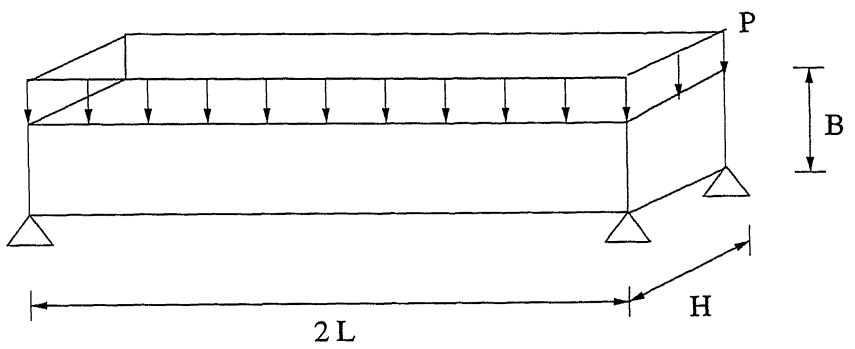

Figure 4 1: Simply supported beam under uniformlly distributed load

Plane strain condition is simulated by applying appropriate boundary conditions. Only a half of the beam is analysed.

Stress-strain relation used is

$$(\sigma_{eq}/\sigma_y) = (E\epsilon_{eq}/\sigma_y)^n \quad \text{for } \sigma > \sigma_y \tag{4 1}$$

Where the material constants are:
Yield stress $(\sigma_y) = 21.5$ N/mm2
Young's modulas $(E) = 2500$ N/mm2
Hardening coefficient $(n) = 0.2$

Dimensions of the beam solved are
Length (L) = 100.0 mm Breadth (B) = 10.0 mm Height (H) = 10.0 mm

The ratio of maximum load to load at yield is plotted against the ratio of maximum deflection to deflection at yield (figure 4.2). The results are in good agreement with theoritical solution provided by Chakrabbrty (figure 4.3).

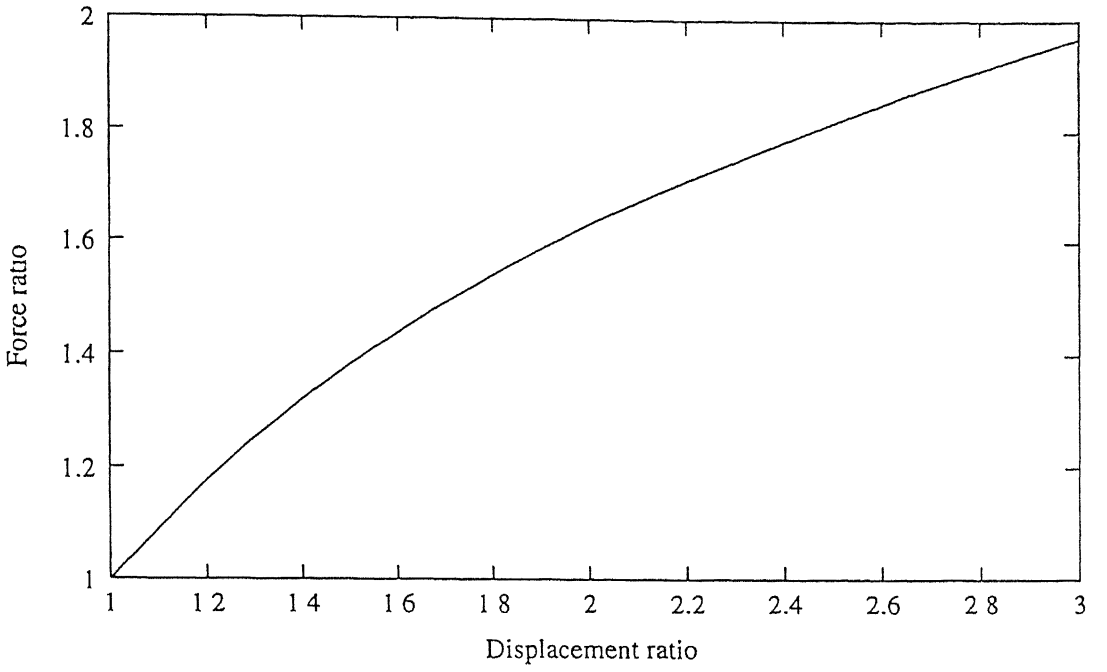

Figure 4.2. Load ratio versus the deflection ratio

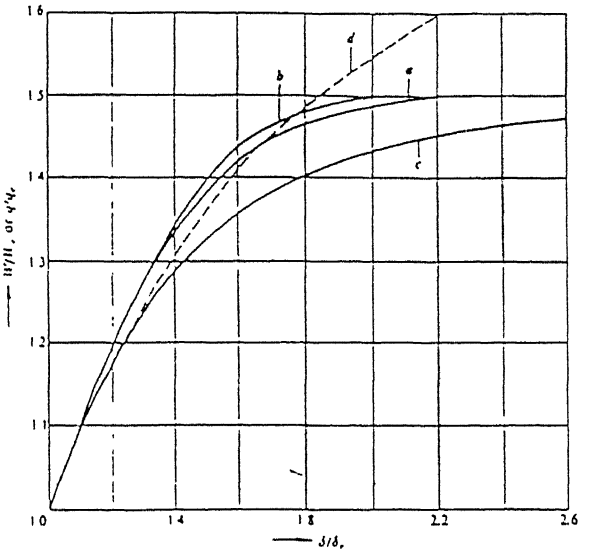

Load-deflection curves for statically determinate beams. (*a*) Cantilever with a terminal load, (*b*) uniformly loaded cantilever (*c*) simply supported and uniformly loaded beam, (*d*) effect of strain-hardening on case (*c*) when $n = 0.2$.

Figure 4 3: Load ratio versus the deflection ratio

4.1.2 Validation of contact part of code

The contact part of the code has been tested with a numerical problem solved in Zhong (1993). The problem consists of two elastic cantilever beams in frictionless contact (figure 4.4).

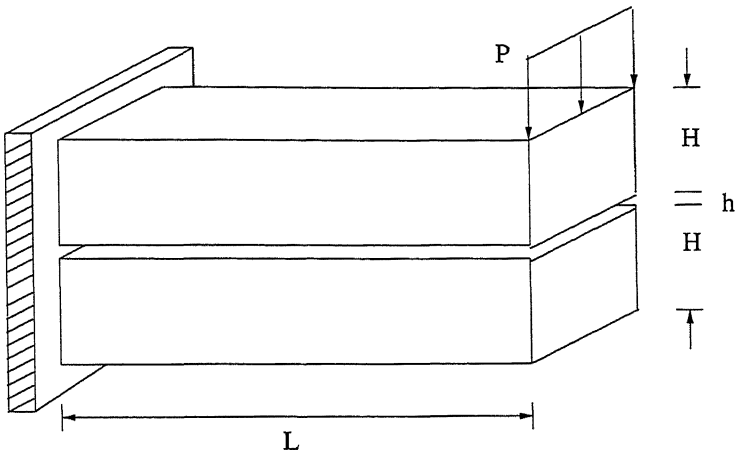

Figure 4.4: A two-beam contact system (P = 80 MN)

Where dimensions are
length (L) = 1.0 m
height (H) = 0.1 m
length (B) = 0.1 m
gap (h) = 0 01 m
Material properties used are:
Young's modulus (E) = 200 GPa
Poissonis ratio = 0.0

Zhong(1993) has solved it as a 2-D plane stress problem. In present analysis plane stress condition is simulated by applying appropriate boundary conditions. The finite element mesh used is shown in figure 4.5. Two elements have been chosen in the direction perpendicular the paper.

The Lagrange multiplier method is used to impose contact constraints. The total load is applied in thirty steps. The two deformed configurations are shown in the figure 4.6 and 4.7.

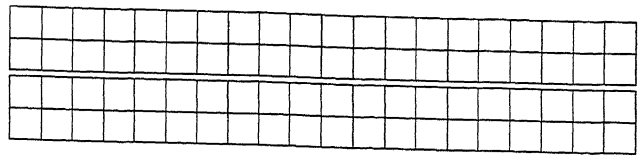

Figure 4.5: A finite element mesh for the beam in contact

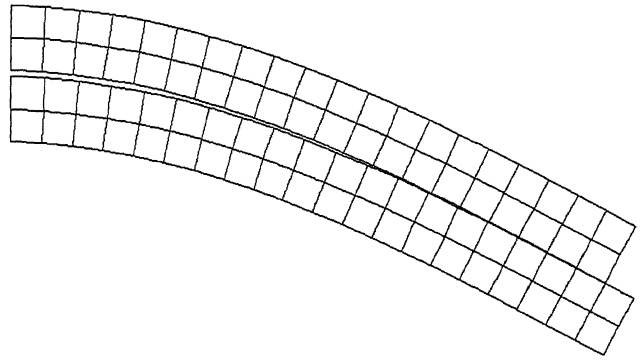

Figure 4.6: Deformed configuration of the beams in contact (Load level-15)

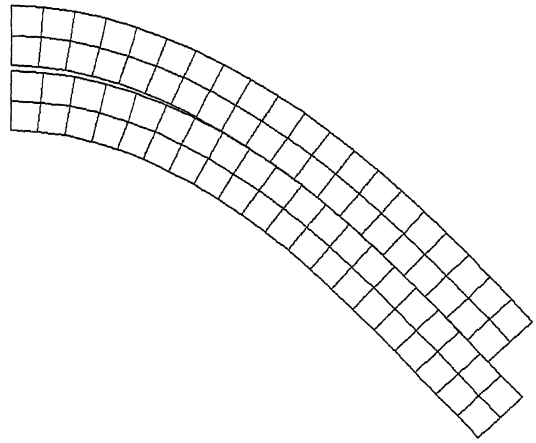

Figure 4.7: Deformed configuration of the beams in contact (Load level-30)

The displacement of the node at which load is applied is plotted against the load level in figure 4.8. The results are in good agreement with the results provided by Zhong (figure 4.9).

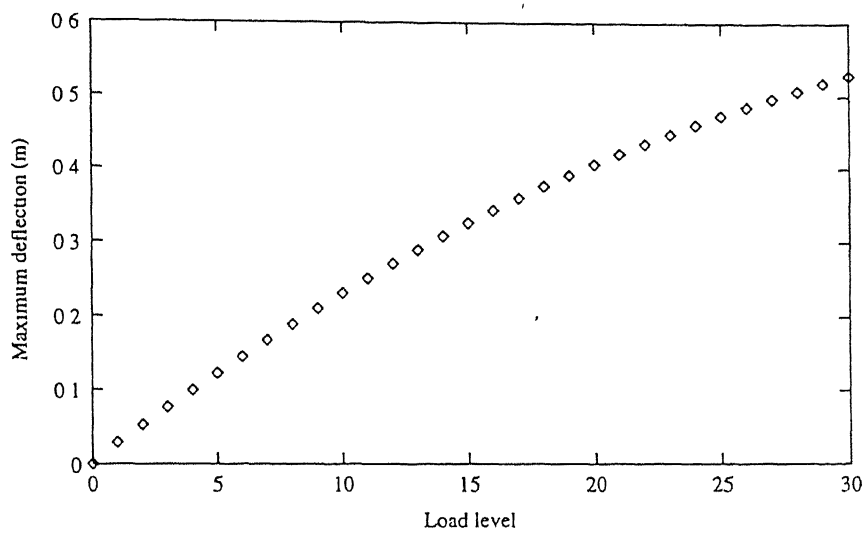

Figure 4 8: The maximum deflection of the upper beam as a function of the load level

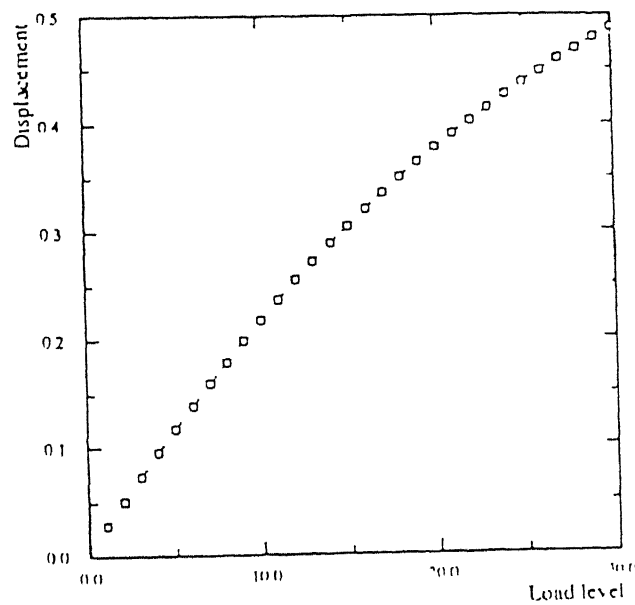

Figure 4.9: The maximum deflection of the upper beam as a function of the load level

4.2 Elasto-plastic contact problem

In this section, an elasto-plastic contact problem between a ball and a plate is solved. Geometry of the contact system is shown in figure 4.10.

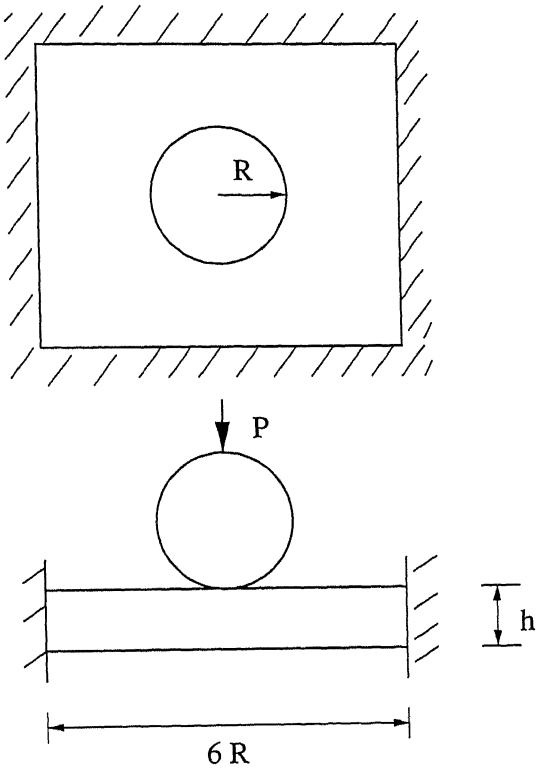

Figure 4.10: Contact system of a ball over a plate (R = 75.00mm, h=20.00mm)

By exploiting the symmety in two perpendicular planes, only a quarter of the domain is analysed. The finite element mesh used, in a plane of symmetry is shown in figure 4.11. For the ball five elements are chosen in the θ direction while for the plate, eight elements are selected in the third direction.

The ball and plate are made of the polycarbonate material. The material properties are:
E (Young's modulus) = 1114.58 N/mm^2
ν (Poisson's ratio) = 0.36
σ_y (Yiled stress) = 44.58 N/mm^2

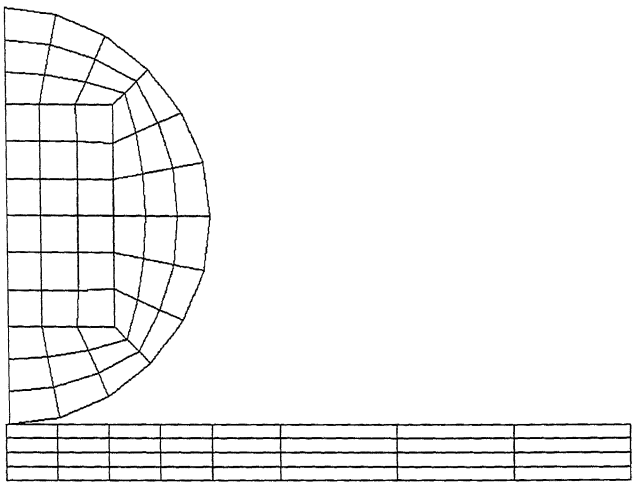

Figure 4.11: Finite element mesh for the ball over plate system
No of nodes for body ball = 100

σ_f (Failure stress) = 82.71 N/mm^2
k (Hardening coefficient) = 87.72 N/mm^2
n (Hardening exponent) = 0.909

Analysis is carried out till the plate fails. The deformed configuration at failure is shown in figure 4.12.

Initialy, only one row of hitting nodes is in contact with the plate. As the load is increased, more and more nodes of the hitting body come in contact with the plate. The maximum deflection occures at the point of application of load while the element just below the applied load is maximally stressed. Figure 4.13 shows the variation of load level versus the maximum deflection.

To study how the contact length varies with different materials, following combinations of materials are used for the ball and the plate.

1. Acrylic ball and acrylic plate

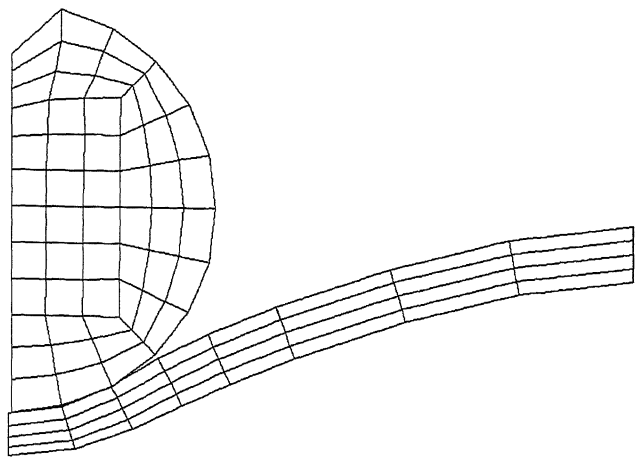

Figure 4.12: Deformed mesh (polycarbonate-polycarbonate)

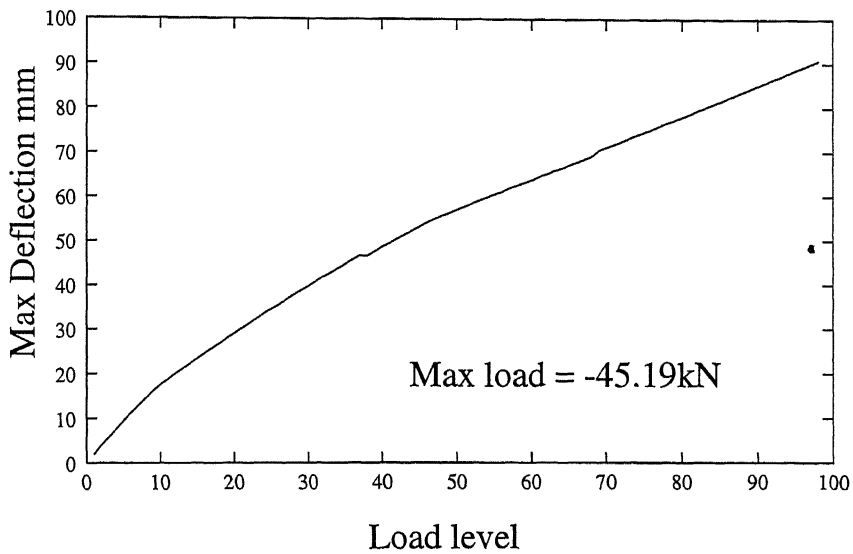

Figure 4.13: Maximum deflection of load point as function of load level (polycarbonates-polycarbonate)

2. Acrylic ball and polycarbonate plate

3. Polycarbonate ball and acrylic plate

The material properties of the acrylic are:

E (Young's modulus) = 2183.99 N/mm^2
ν (Poisson's ratio) = 0.35
σ_y (Yiled stress) = 21.5 N/mm^2
σ_f (Failure stress) = 73.39 N/mm^2
k (Hardening coefficient) = 1408.6 N/mm^2
n (Hardening exponent) = 1.01

Figures 4.14, 4 15 and 4.16 show the deformed configurations at failure for different material combinations. From these figures, one can see that in the case of acrylic-acrylic combination only one row of hitting nodes come in contact while for the other two combinations, two rows of hitting nodes come in contact. Figures 4.17, 4.18 and 4.19 are the plots of load level against maximum the deflection. It is found that in case of acrylic-acrylic and polycabonate-acrylic combinations plate fails before the ball while in polycarbonate-polycabonate and acrylic-polycarbonate cases the ball fails before the plate. From the load deflection plots, one can see that curve is more stiffening for the case of polycarbonate-polycarbonate (4.13) and acrylic-polycarbonate (4.18) combination. This is due to the fact that though the deflection is more in these cases, the plastic deformation zones are smaller than the other two cases. This may be attributed to the fact that the yield stress of polycabonate is large than of acrylic, hence many points do not yield.

One of the important objectives of an analysis of a contact problem is to determine the contact stress distribution. A fine mesh is required in the contact region for accurate estimation of the contact stresses. In this work, the refinement of mesh in the contact region can not be carried out due to difficulties involved in generation of a large 3-D mesh.

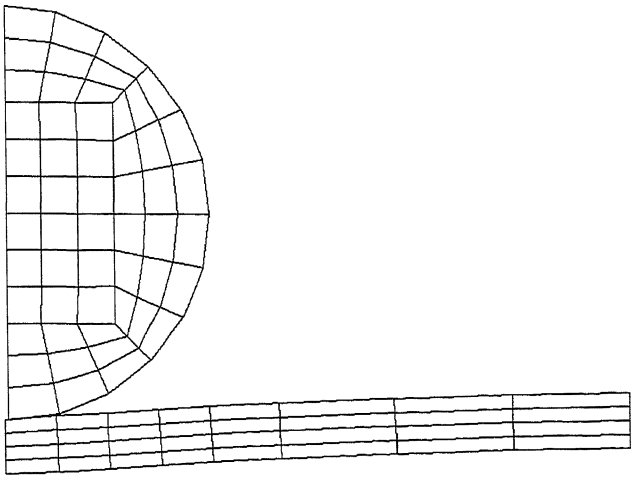

Figure 4.14: Deformed mesh (acrylic-acrylic)

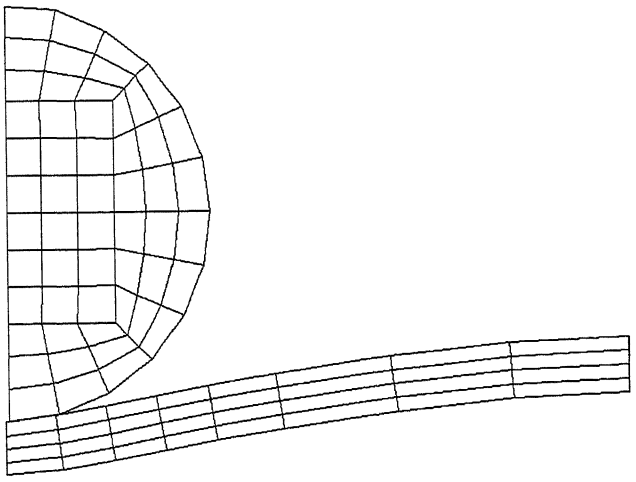

Figure 4.15: Deformed mesh (acrylic-polycarbonate)

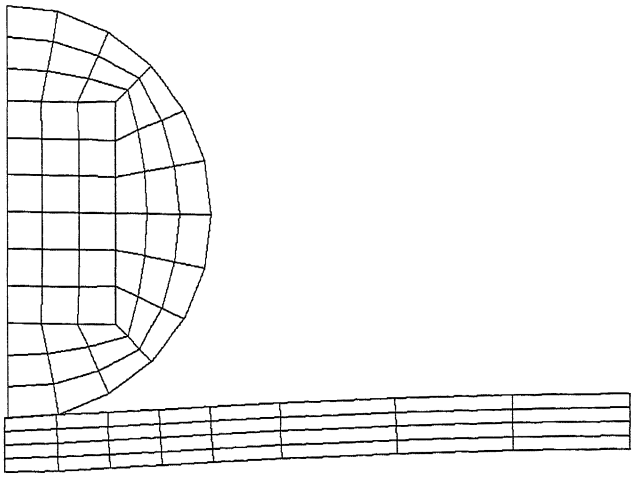

Figure 4.16: Deformed mesh (polycarbonate-acrylic)

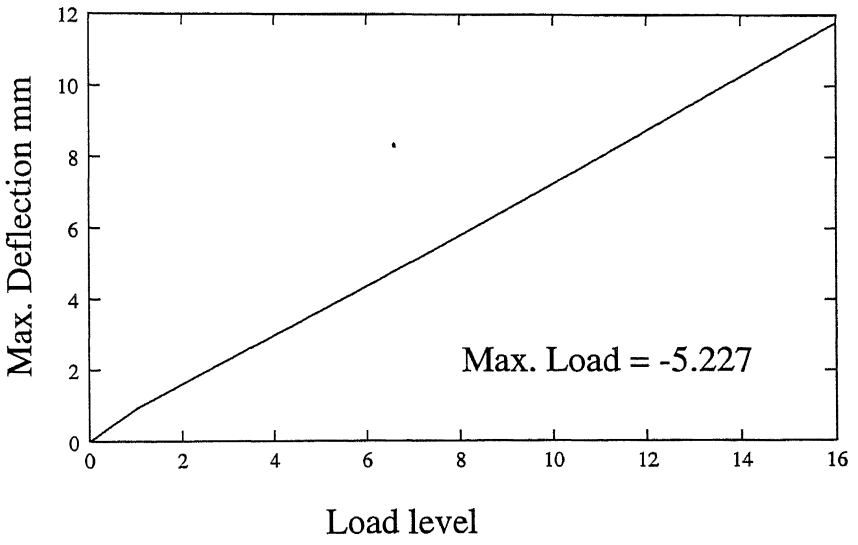

Figure 4.17: Maximum deflection of load point as function of load level (acylic-acylic)

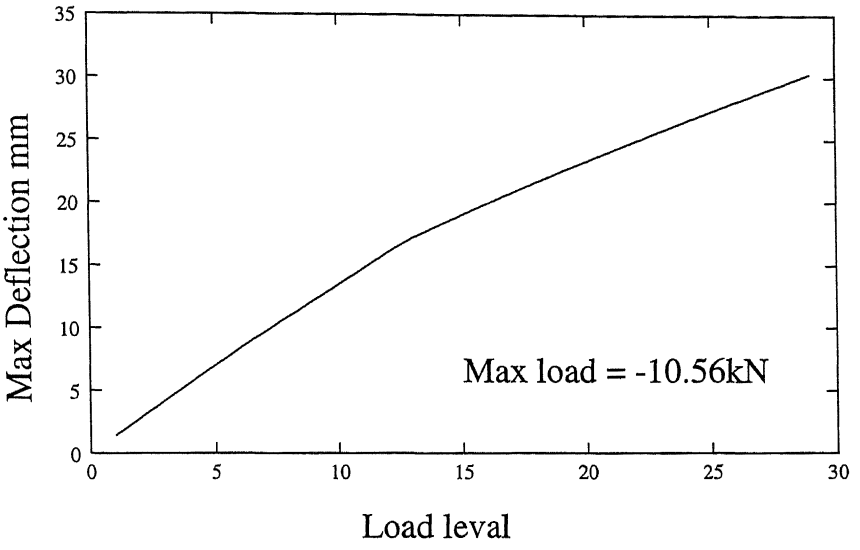

Figure 4.18: Maximum deflection of load point as function of load level (acrylic-polycarbonate)

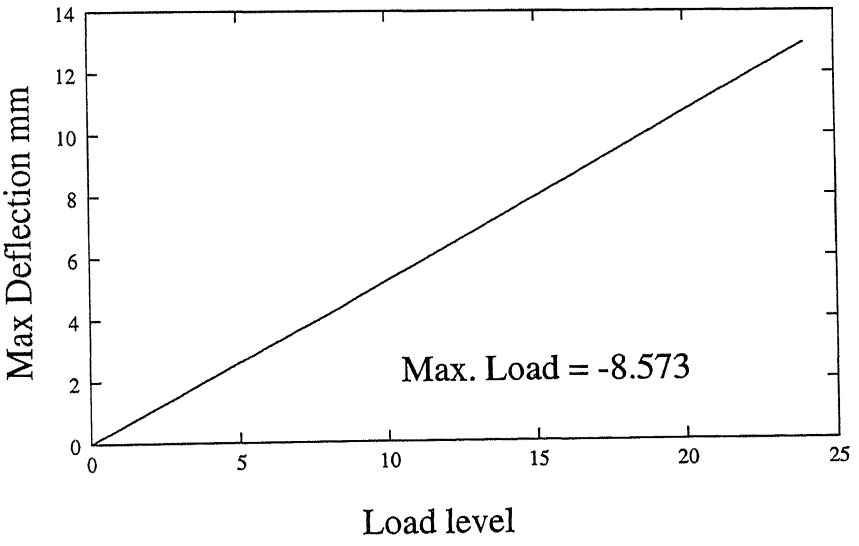

Figure 4.19: Maximum deflection of load point as function of load level (poylcabonate-acrylic)

Chapter 5

Conclusions and Scope for Future Work

5.1 Conclusions

A finite element code has been developed for solving 3-d large deformation elasto-plastic frictionless contact problems. A node-to-segment inerface model is used for developing the contact stiffness matrix. The Langrage multiplier method is used for inforcing the contact constraints. The updated Langrangian formulation along with modified Newton-Raphson iterative scheme is used for carrying out the incremental analysis of the elasto-plastic deformation.

The code has been validated by solving a few test problems. Finally, a 3-D problem (of contact between a ball and plate) is solved for different combinations of contacting materials. The result seems reasonable. This shows that the method can be used successfully for solving 3-d large deformation elasto-plastic (frictionless) contact problems.

5.2 Scope for Future Work

The present can be extended in the following directions :

- Friction effects can be included. This involves modification of the contact stiffness matrix.

- To include the code for solving impact problems, dynamic (inertial) effects should be included. A finite difference scheme needs to be incorporated to tackle the dynamic terms.

- An effective pre-processor should be added to the code so that the problems with complicated geometry can be solved. a versatile post-processor is also desirable to represent the displacement and strss fields in the contact region.

Bibliography

[1] Bathe, K. J. (1990,1996), *"Finite Element Procedures,"* Prentice Hall of India, New delhi.

[2] Bathe, K. J. and Chaudhary, A., (1985), *"A Solution Method for Planar and Axisymmetric Contact Problems,"* Int. J. for. Numerical Methods in Engg., 9, 353-86.

[3] Bathe, K. J., Ramm, E., and Wilson, E., (1975), *"Finite Element Formulations for Large Deformation Dynamics Analysis,"* Int. J. for Num. Methods in Engg., 17, 1823-33.

[4] Chakrabarty, J., (1987), *"Theory of Plasticity,"* McGraw Hill, New York.

[5] Chaudhary, A. and Bathe, K. J., (1986), *"A Solution Method for Static and Dynamics Analysis of Three-dimensional Contact Problems with Friction,"* Computer and Structure, 24, (6), 855-77.

[6] Chen, W. and Yeh, J., *"Finite Element Analysis of Finite Deformation Contact Problems with Friction,"* Comp. and struct., 29 (3), 423-436, (1988).

[7] Francavilla, A. and Zienkiewicz, O. C., (1975), *"A note on Numerical Computation of Elastic Contact Problems,"* Int. J. for Num. Methods in Engg., 9, 913-24.

[8] Gaertner, R., (1977), *"Investigation of Plain Elastic Contact allowing for Friction,"* Comp. Struct., 7, p 59.

[9] Gallego, F. J. and Anza, J. J., *"A Mixed Finite Element Model for Elastic Contact Problem,"* Int. J. for Num. Meth. in Engg., 28, 1249-1264, (1989).

[10] Gladwell, G. M. L., (1980) *"Contact Problems in the Classical Theory of Elasticity,"* Sijthoff & Noordhoff, The netherlands.

[11] Hallquist, J. O., Goudreau, G. L. and Benson, D. J., (1985), *"Sliding Interfaces with Contact-Impact in Large Scale Lagrangian Computations,"* Comp. Meth. in Appl. Mech. and Engg., 51, 107-37.

[12] Hertz, H., (1882), *"On the Contact of Elastic Solids,"* Jr. of Math., 92, p 156 (in German).

[13] Hung, N. D., Sauxe, G., (1980), *"Frictionless Contact of Elastic Bodies by Finite Element Method and Mathematical Programming Technique ,"* Computers and Structure ., 11, 55-67.

[14] kalker, J. J. and Randen, Y., (1979) *"A Minimum Principle for Frictionless Elastic Contact with Application to Non-Hertzian Half- space Contact Problem,"* Jr. Engg. Math., 6, p 193.

[15] Kikuchi, N. and Oden, J. T., (1988) *"Contact Problem in Elasticity, A study of Variational Inequality and Finite Element Methods,"* SIAM, Philadelphia.

[16] Mahmoud, F. F., Al-Saffer,A. K. and El-Hadi, A. M. (1991) *"Solution of the Non-conformal Unbounded Contact Problems by the Incremental Convex Programming Method,"* Comp. struct., 39, p 1.

[17] Muskhelishvili, N. I., (1975) *"Some Basic Problems of the Mathematical Theory of Elasticity,"* Noordhoff, The netherlands.

[18] Ohte, S., (1973), *"Finite Element Analysis of Elastic Contact Problem ,"* Bulletin of JSME., 16, 798-804.

[19] Owen, DRJ.and Hinton, E. *"Finite Elements in Plasticity : Theory and Practice,"* Pineridae Press Ltd., UK.

[20] Parisch, H., (1989), *"A Consistent Tangent Stiffness Matrix for Three-dimensional Non-linear Contact Analysis,"* Int. J. of Num. Meth. in Engg., 28, 1803-12.

[21] Sachdeva, T. D. and Ramakrishnan, C. V., (1981), *"A Finite Element Solution for the Two-dimensional Elastic Contact Problems with Friction ,"* Int.J.of Num. Meth. in Engg.

[22] Wriggers, D. and Simo, J. C., (1985), *"A Note on Tangent Stiffness for Fully Non-linear Contact Problems,"* Comp. in Appl. Num. Meth., 199-203.

[23] Wriggers, P., Van, T. V. and Stein, E. *"Finite Element Formulations of Large Deformation Impact-Contact Problems with Friction,"* Comp. and Struct., 37 (3), 319-331, (1990).

[24] Zhong, Zhi-Hua, *"A Finite Element Procedures for Contact-impact Problems,"* Oxford University Press, (1993).

[25] Zboinski, G., *"A Finite Element Algorithm for Incremental Analysis of Large Three-dimensional Frictional Contact Problems of Linear Elasticity,"* Comp. and Struct., 46 (4), 669-677, (1993).